Simulations of viscous shape relaxation in shuffled foam clusters

Gilberto L. Thomas, José C.M. Mombach, Marco Idiart, Catherine Quilliet, François Graner

Simulations of viscous shape relaxation in shuffled foam clusters

Gilberto L. Thomas[1], José C.M. Mombach[2], Marco A. P. Idiart[1],
C. Quilliet[3], F. Graner[3]

[1] Instituto de Física, Universidade Federal do Rio Grande do Sul,
C.P. 15051, 91501-970 Porto Alegre, Brazil.
[2] Laboratório de Bioinformática e Biologia Computacional
Centro de Ciências Exatas e Tecnológicas, Universidade do Vale do Rio dos Sinos,
Av. Unisinos, 950 93022-000 São Leopoldo, RS, Brazil
[3] Laboratoire de Spectrométrie Physique, BP 87, 38402 St. Martin d'Hères Cedex, France.

Abstract

We simulate the shape relaxation of foam clusters and compare them with the time exponential expected for Newtonian fluid. Using two-dimensional Potts Model simulations, we artificially create holes in a foam cluster and shuffle it by applying shear strain cycles. We reproduce the experimentally observed time exponential relaxation of cavity shapes in the foam as a function of the number of strain steps. The cavity rounding up results from local rearrangement of bubbles, due to the conjunction of both a large applied strain and local bubble wall fluctuations.

Keywords: **two-dimensional foam cluster, cellular fluid, hydrodynamic relaxation, Potts model.**

1 Introduction

Liquid foams, and especially two-dimensional ones, are easy to image and manipulate, and hence can be a quite efficient model for other complex systems [1] and, in particular, for biological cell aggregates [2, 3, 4].

Biological cell aggregates and foams share a common point: they are "cellular fluids"; they can flow while their constituent cells rearrange and change neighbors through relative local movements [1]. When out of equilibrium, their mechanical behavior displays elastic, plastic or viscous responses.

Interestingly, the rounding up of cell aggregates observed in biology is similar to the coalescence or rounding up of liquid droplets. Gordon *et al.* [5] made a formal analogy with the rheology of viscous liquids, showing that tissue surface tensions drive these processes, while tissue viscosity resists them. Recently, Rieu and Sawada [6] showed that a hydrodynamic laws also apply to the rounding-up of two-dimensional (2D) aggregates of mixed ectodermal and endodermal *hydra* cells in various proportions. They obtained time-exponential relaxations for rounding up of aggregates. Corresponding simulations [7] have investigated the relaxation of biological cell aggregates of elliptical shapes.

What is common between the relaxation of biological cell aggregates and foams, and how does it differ from that of an usual Newtonian fluid? To address this question, the companion paper [8] studies the relaxation of a foam cluster, and in the present paper we perform the corresponding simulations using Cellular Potts Model [2, 9] .

Concerning the mechanism of relaxation a foam has an important difference with biological cell aggregates. Cell membranes fluctuate actively, with a r.m.s. movement equivalent to that produced by a very high effective temperature (much higher than room temperature); so that cells explore their neighborhood and can move. The macroscopic configuration of a foam, on the other hand, arises from the local equilibrium of the bubbles' surface tensions

and pressures. A foam never reaches its global energy minimum since the energy barriers between local equilibrium states, attainable by moving passive bubbles around, are much higher than the order k_BT thermal energy fluctuations at room temperature. At bubble scales, we can consider a foam to be at zero temperature, so that the foam configuration falls and is trapped in an energy minimum; we do not expect to observe rounding up of foams at room temperature.

In order to circumvent that we introduce energy in the foam through successive shear cycles [8, 10]. The external force shears the foam, rearranging bubbles, and exploring new energy configurations, and relaxing into more stable configurations. Our goal is to determine if the relaxation laws we obtain by this method are the same as those for aggregates of biological cells, *i.e.*, if mechanical stimulation is equivalent to an effective temperature. However, experimentally, applying external mechanical strain turned much easier for foam cluster with a hole in it (Fig. 1) than for a cluster which does not touches the box walls. Thus we address here the cavity relaxation, as if it was the "negative" of the aggregate relaxation [6, 7]. We also study the center of mass movement of cavities of different sizes in the foam to compare with the experimental observations in [8].

2 The Model

The 2D model reflects the quasi-2D experimental foam of Ref. [8], see Fig. 1. We use the extended large-Q Potts model, which allows large numbers of bubbles, fixed bubble areas, and large foam distortions [11]. This model represents the spatial structure of the foam as follows. We consider a 2D square grid. The model treats a foam on a 2D lattice by assigning an integer index to each lattice site. The value at a grid site (i, j) is σ if the site lies inside bubble σ. Each bubble of the foam is thus the connected set of grid sites with the same index σ. Each bubble is thus labelled by this index σ and occupies many grid sites.

Each pair of neighbors having unmatched indices determines a bubble wall and contributes to the bubble wall surface energy. The prefactor J is the surface tension (which we can here take equal to 1 without loss of generality). Bubble areas are the number of lattice sites for each index; an area constraint keeps the bubble areas constant. The actual bubble area is $A(\sigma)$ and the target bubble area is A_t, the same for each bubble. The prefactor λ is the compressibility of the bubble. The Hamiltonian thus writes:

$$H = \sum_{(i,j),(i',j')} J(\tau(\sigma(i,j)), \tau'(\sigma'(i',j')))(1 - \delta_{\sigma(i,j),\sigma'(i',j')}) + \sum_{\sigma} \lambda(\tau)(A(\sigma) - A_t)^2 \ . \qquad (1)$$

Here the second sum is over all bubbles, while the first sum is over all pairs of neighboring sites of coordinates (i, j) and (i', j'). We use the 5th nearest neighbors to decrease the effect of the anisotropy of a discrete lattice [12]. $J(\tau(\sigma(i, j)), \tau'(\sigma'(i', j')))$ denotes the interaction energy between the neighboring sites (i, j) and (i', j'). We treat the cavity as a large single bubble; we thus introduce the index τ which is the bubble type: the cavity has $\tau = 0$, while all the bubbles are of type $\tau = 1$. Since all bubbles have a fixed area, and the total area is fixed too, a constraint on the cavity would be redundant (leading to numerical instabilities), so we do not enforce it (we set $\lambda(0)$ to 0).

Energy minimization through Metropolis dynamics [2, 9] minimizes the total wall energy (sum of bubble perimeters). In the Monte Carlo dynamics, at each step, we select a random grid site (i,j). An attempt to change its index from σ to σ ' is tried (where σ ' is the index of an

arbitrary lattice site among one of its first neighbors) and is performed with the probability,:

$$P(\sigma(i,j) \to \sigma'(i,j)) = \begin{cases} \exp(-\Delta H/kT) & \text{if } \Delta H > 0, \text{ or} \\ 1 & \text{if } \Delta H \leq 0, \end{cases} \quad (2)$$

where ΔH is the energy gain the change produces. Each such move corresponds to bubble σ' displacing bubble σ by one lattice site. $T > 0$ is a fluctuation temperature corresponding to the amplitude of bubble wall fluctuations. The time unit, a Monte Carlo step (MCS), corresponds by definition to as many attempts as the number of lattice sites.

3 Cavity relaxation

Simulations run on square grid containing about 20 x 20 bubbles of the same size (either 63 or 99 lattice sites), with a centered cavity whose size we measure in number of bubbles (ratio of cavity area to bubble area).

To shear the foam, we proceed in the following way; which closely mimics the experimental set-up (Fig. 1). From the initial state, we periodically displace the lower part of the grid horizontally up to the desired maximum angle, and in the opposite direction as well. We slide each row by interpolating between the lower (moving) and upper (fixed) sides. This procedure distorts each bubble, which can change its shape and its neighbors. Then we allow the foam to relax.

We observed that, at all angles we tried (up to 30°), at zero temperature this procedure alone does not cause rounding. Therefore at each position shown in Fig. 1 we relax at finite temperature for 100 MCS, then anneal at $T = 0$ for the same amount of time. We choose a temperature small enough so that the thermal treatment by itself does not cause rounding. Since one shear cycle is performed in four such sub-steps, it takes 800 MCS.

Defining the cavity eccentricity as $e = 1 -$ minor axis/major axis, Fig. 2 shows the relaxation for different maximal displacement angles. We chose two different initial cavity shapes: both shapes (rectangular and ellipsoidal) have the same behavior. Higher shear result in quicker relaxation. In all cases, the semi-log plot is close to a straight line: the relaxation is close to exponential in time, enabling us to define a characteristic time (τ_c).

Fig. 3 shows τ_c for rounding of foams with two different bubble sizes (63 and 99 lattice sites), but with the same cavity / bubble size ratio, and for different maximal angles. Rounding is faster for larger bubbles and for larger maximal angles.

We have also investigated the behavior of cavities of different sizes. Fig. 4 shows a large variation in cavity sizes. Initially the rounding is exponential, but it later slows down, especially for small cavities for which it saturates, in agreement with Ref. [8]. Fig. 5 shows the rounding characteristic time for this situation. We can see that smaller cavities round faster.

4 Cavity diffusion

Motivated by the experimental observations [8], we performed a set of measurements to investigate the diffusion of the cavity as a result of both shearing and increasing the temperature. Fig. 6 shows the cavity center of mass position during shear cycles for different cavity sizes. As expected, the smaller the cavity, the more it moves.

To test whether this movement corresponds to a diffusion, Fig. 7 displays the quadratic center of mass displacement for the same cavity sizes. The answer is no: we do not observe any significant diffusion. The same holds if we increase the deformation angle (Fig. 8).

5 Summary

Cavities of different shapes round similarly. The combination of deformation and finite temperature annealing in our simulations reproduces the exponential relaxation behavior of rounding up of biological cell aggregates. Our results have also shown that rounding is faster for larger maximal sheared angles, for cavities in foams with larger bubbles and for cavities with smaller sizes. Neither temperature, in the range we choose, nor shearing alone causes rounding. The finite temperature annealing in the simulation might represent some other form of energy transfer, present in the experiment, for example vibration of the foam during mechanical shearing. No evidence suggests that shearing the system induces diffusion.

The next step in our investigation is to study, by experiments and simulations, single bubble movement during shearing. If periodic shearing represents an input of energy equivalent to a thermal bath of finite temperature, individual bubbles could diffuse, even if the cavity does not.

Acknowledgements

Capes–Cofecub exchange project No. 414/03 supported this work. J. C. M. Mombach acknowledges the partial support of HP Brazil R&D.

References

[1] D. Weaire and S. Hutzler. *The physics of foams*, Oxford University Press, New York, 1999.

[2] J.A. Glazier and F. Graner. *Phys. Rev. E* **47**, 2128 (1993).

[3] H. Honda, M. Tanemura, and T. Nagai. *J. theor. Biol.* **226**, 2128 (1994).

[4] B. Dubertret and N. Rivier. *Biophys. J.* **73**,38 (1997); N. Rivier, M.F. Miri, and C. Oguey. Article in this volume.

[5] R. Gordon, N. S. Goel, M. S. Steinberg, and L. L. Wiseman. *J. Theor. Biol.* **37**, 43 (1972).

[6] J.-P. Rieu and Y. Sawada. *Eur. Phys. J.* **B 27**, 167 (2002).

[7] J.C.M. Mombach, D. Robert, F. Graner, G. Gillet, G.L. Thomas, M.A.P. Idiart, J.-P. Rieu. Submitted for publication.

[8] C. Quilliet, M. Idiart, B. Dollet,L. Berthier, and A. Yekini. *Bubbles in sheared two-dimensional foams.* Article in this volume.

[9] F. Graner and J.A. Glazier. *Phys. Rev Lett.* **69**, 2013 (1992).

[10] V. Viasnoff, S. Jurine, and F. Lequeux. *Faraday Discuss.* **123**, 253 (2003).

[11] Y. Jiang, P. J. Swart, A. Saxena, M. Asipauskas, and J. A. Glazier, Phys. Rev. E **59**, 5819 (1999).

[12] E. Holm, J. A. Glazier, D. J. Srolovitz, and G. S. Grest, Phys. Rev. A **43**, 2262 (1991).

Figures

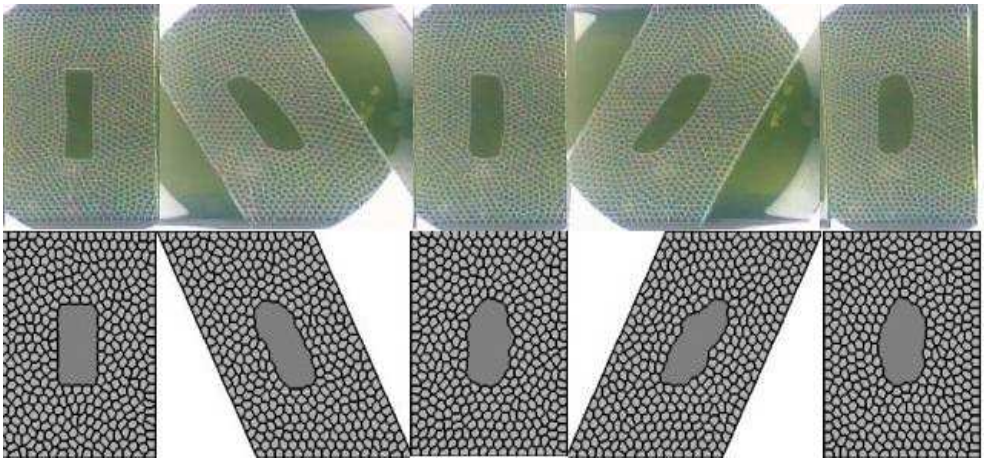

Fig. 1

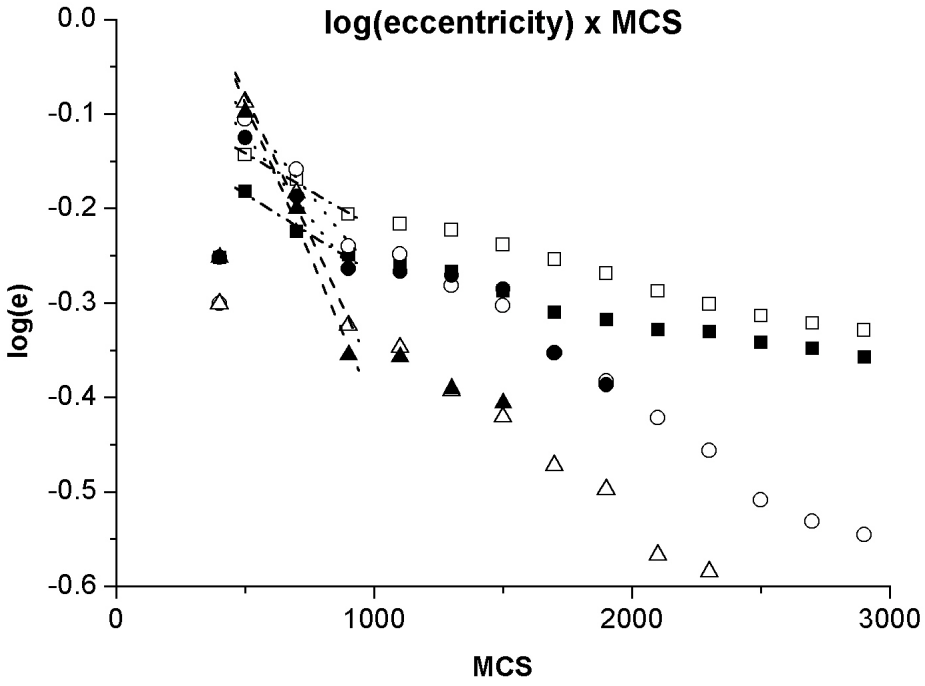

Fig. 2

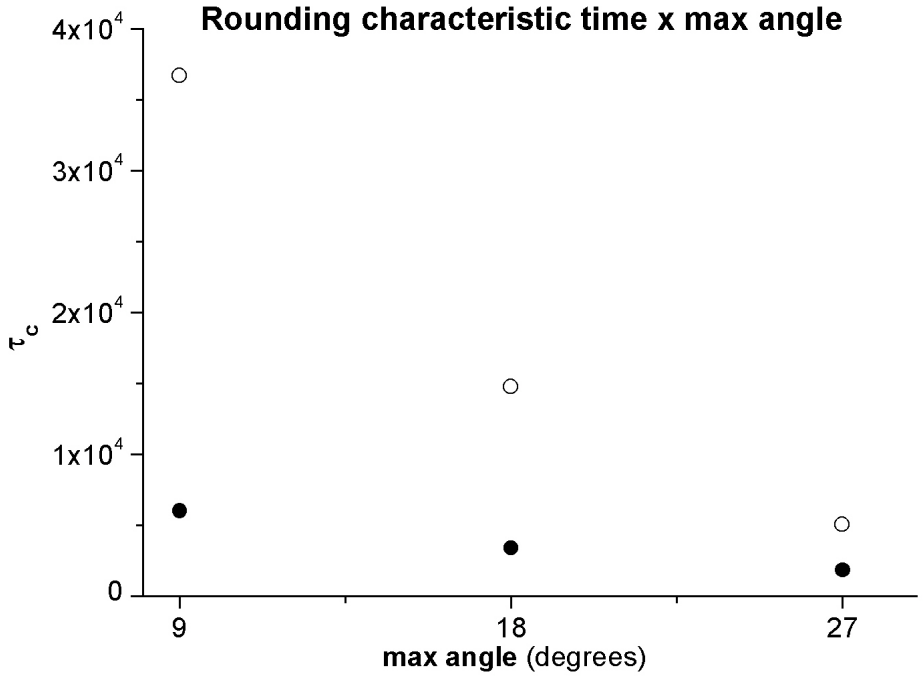
Rounding characteristic time x max angle
4x10^4
3x10^4
2x10^4
1x10^4
0
τc
9
18
27
max angle (degrees)

Fig. 3

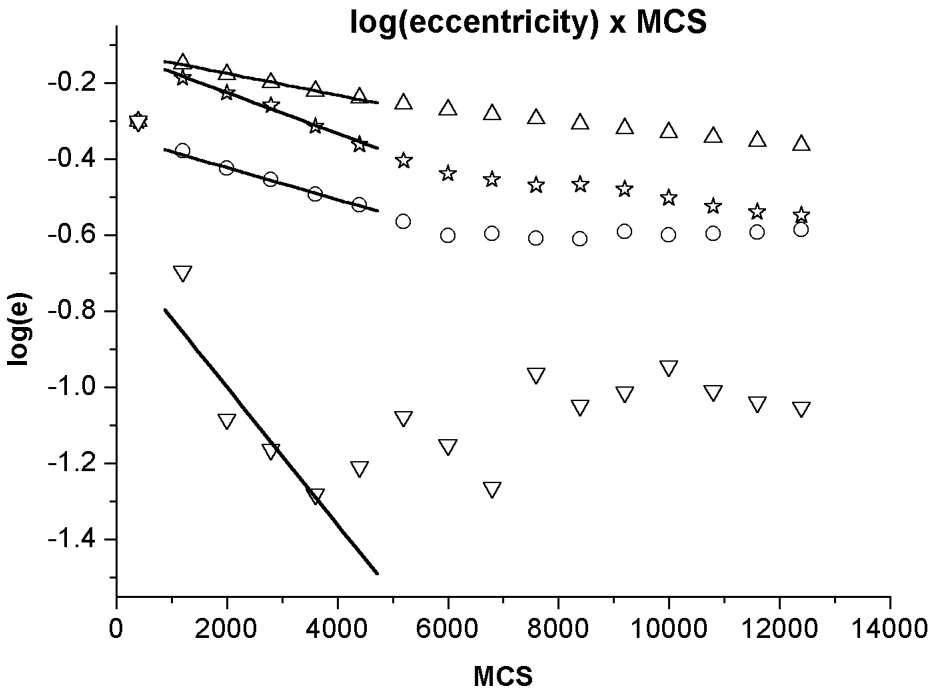
log(eccentricity) x MCS
-0.2
-0.4
-0.6
-0.8
-1.0
-1.2
-1.4
log(e)
0
2000
4000
6000
8000
10000
12000
14000
MCS

Fig. 4

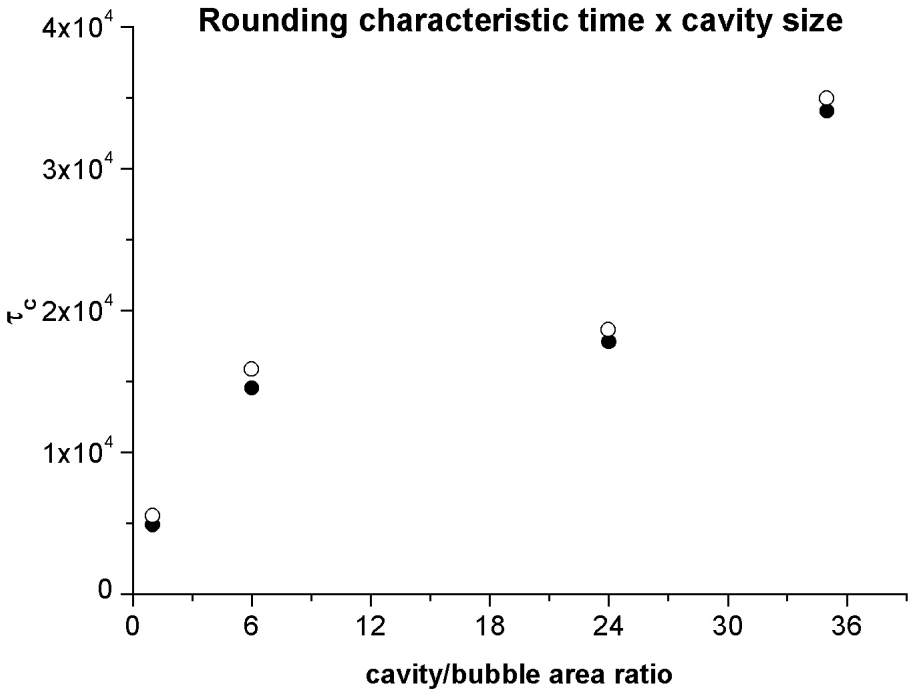
Rounding characteristic time x cavity size
4x10^4
3x10^4
2x10^4
1x10^4
0
τc
0
6
12
18
24
30
36
cavity/bubble area ratio

Fig. 5

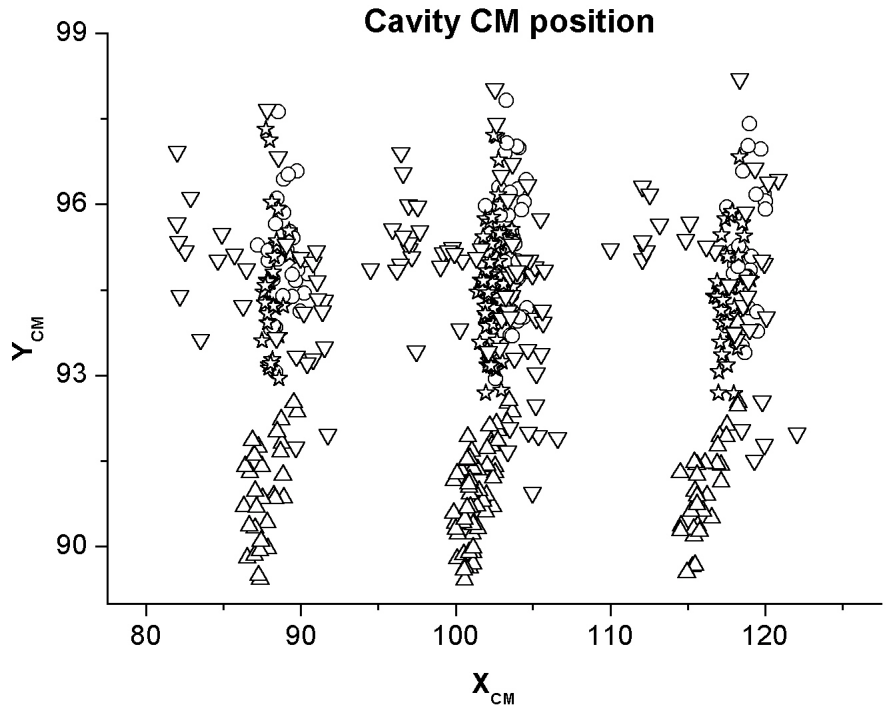
Cavity CM position
99
96
93
90
YCM
80
90
100
110
120
XCM

Fig. 6

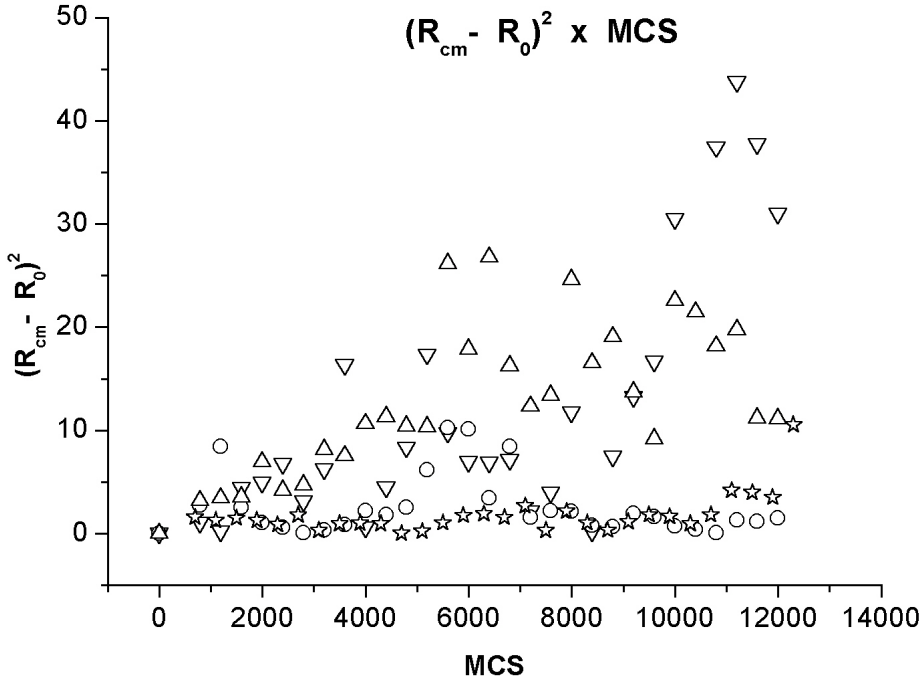
$(R_{cm} - R_0)^2$ x MCS
$(R_{cm} - R_0)^2$
MCS
0
10
20
30
40
50
0
2000
4000
6000
8000
10000
12000
14000

Fig. 7

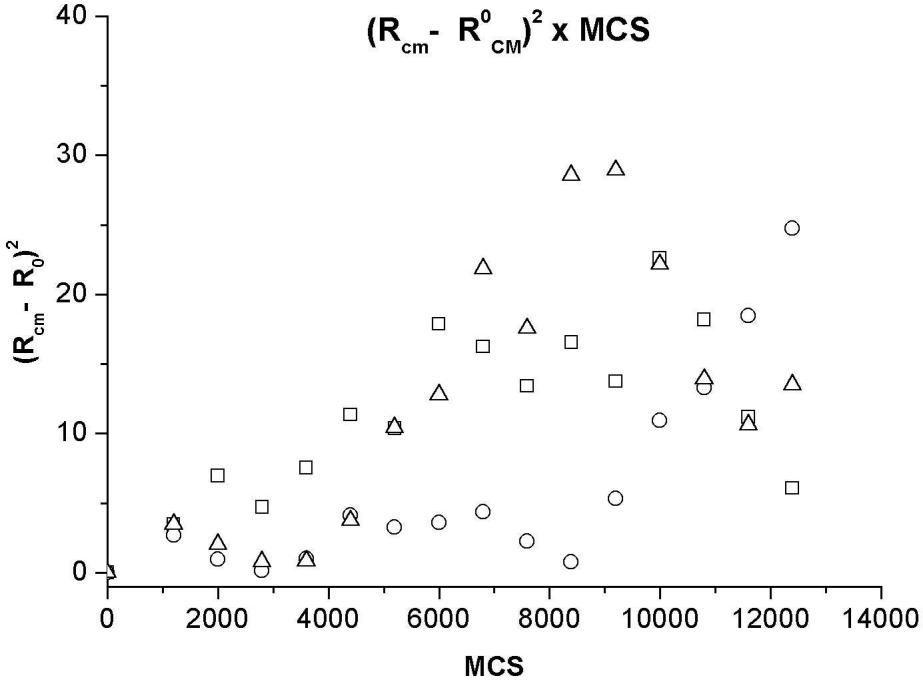
$(R_{cm} - R^0_{CM})^2$ x MCS
$(R_{cm} - R_0)^2$
MCS
0
10
20
30
40
0
2000
4000
6000
8000
10000
12000
14000

Fig. 8

Figure captions

Fig. 1 One shear cycle, here with initially rectangular cavity. Top: experimental setup [8]. The foam is sheared back and forth, to the maximal angle, in both directions. Bottom: corresponding simulation (bubble size = 63 lattice sites).

Fig. 2 Time relaxation of cavity shape: $\log(e)$ *versus* time (MCS) for different maximal angles. After a transient, both rectangular and ellipsoidal cavities round similarly. Shear is labelled by the maximal deformation angle: 9, 18 or 27°.

Fig. 3 Characteristic relaxation time τ_c *versus* maximal shear angle for two different bubble sizes: 63 lattice sites (open circles) and 99 lattice sites (closed circles).

Fig. 4 Cavity relaxation: $\log(e)$ *versus* time (MCS) for very different cavity area / bubble area ratios: 1 (inverted triangle), 6 (circle), 24 (star) and 35 (triangle). Bubble size = 63, elliptical initial cavity, deformation angle 9°.

Fig. 5 Characteristic relaxation time τ_c *versus* cavity size. Bubble area is fixed to 63; elliptical initial shape; deformation angle 9°. Note that if we consider all data taken at half cycles (closed circles) we obtain the same results as if we perform measurements only at integer cycles (open circles).

Fig. 6 Cavity center of mass position for different cavity area / bubble area ratios: 1 (inverted triangle), 6 (circle), 24 (star) and 35 (triangle). Bubble size = 63, elliptical initial cavity, deformation angle 9°. Note the difference in horizontal and vertical scales.

Fig. 7 Center of mass displacement $(R_{CM} - R_o)^2$ *versus* time (MCS) for different cavity area / bubble area ratios: 1 (inverted triangle), 6 (circle), 24 (star) and 35 (triangle). Bubble size = 63, elliptical initial cavity, deformation angle 9°.

Fig.8 Center of mass displacement $(R_{CM} - R_o)^2$ *versus* time (MCS) for different maximal sheared angle: 9 (square), 18 (circle) and 27°(triangle). Cavity area / bubble area ratio = 35, bubble size = 63, elliptical initial cavity.